# HIGH-FIELD CAPTURE SECTION FOR SLC POSITRON SOURCE*

H. A. HOAG, H. DERUYTER, J. KRAMER AND C. G. YAO
*Stanford Linear Accelerator Center, Stanford, California 94305*



## Introduction

The positron source for SLC is being installed at the two-thirds point on the SLAC linac. Electron bunches at 33 GeV impinge upon a Tantalum/Tungsten target, producing showers of positrons with energies[1] extending from approximately 2 to 20 MeV, with most positrons at the low end of this range. Positrons with low energies and finite transverse momenta slip phase during the processes of reacceleration and reinjection into the SLC system, increasing the energy spread and reducing the overall yield of the positron source. This reduction in yield has to be minimized by "capturing" the positrons with a high-field accelerator section placed as soon after the target as possible. The design, fabrication and RF testing of this accelerator section is the subject of this paper.

## Choice of Structure

At the outset, we were confronted with the task of choosing between traveling-wave (TW), standing-wave (SW) and recirculating (R) modes of operation in a disk-loaded circular waveguide (DLWG), which could be singly or multiply periodic. In the interests of schedule and budget, there was a bias towards using a short section of DLWG, either Constant Gradient (CG) or Constant Impedance (CI), in the TW mode, since techniques for building such a structure are well-known at SLAC.

Drawing principally from the work of G. A. Loew and R. B. Neal,[2] a simple comparative study of the expected beam energies was made for each of the three modes of operation mentioned above. For the study, a 29-cavity CI DLWG (1.015 meters long) was used. Energies were calculated for five different disk aperture diameters. In all cases, operation in the $2\pi/3$ mode was assumed, with a 50 MW klystron driving the section through a rectangular WG feed with 0.97 dB loss. Figure 1 shows that, as expected, the energies theoretically obtainable with recirculating and standing-wave operation exceed those reached under traveling-wave conditions.

However, it was very clear that the possibilities of the SLED-[3] pulse compression system should be explored. It quickly became apparent that the combination of a SLEDed klystron with a simple, short CI TW DLWG section is a very good way of obtaining high accelerating fields - see the top solid curve in Fig. 1. The short filling time $T_f$, the constant attenuation $\alpha$ per unit length, and the small attenuation parameter $\tau$, (where $\tau = \alpha L$, and $L$ is the section length), have several beneficial effects:

- Practically the whole klystron RF pulse width (5 $\mu$s in our case) is available to charge the SLED cavities, giving a large pulse-compression ratio.
- At beam injection time (when the section is just filled with RF energy), the field in the input cavity is still high, since the section filling time is short compared to the SLED cavity filling time. Moreover, the time-decay of the incoming SLED peak field approximately matches the spatial attenuation of the field propagating along the structure. Thus when the beam passes through the capture section it interacts with a nearly constant voltage gradient, as can be seen from the cavity field curves in Fig. 1.
- The short duration of the high field pulse may not allow time enough for development of some sparking mechanisms, such as surface heating due to multipactor, surface gas desorption due to heating and electron bombardment, and local gas ionization leading to plasma discharge and avalanche breakdown.

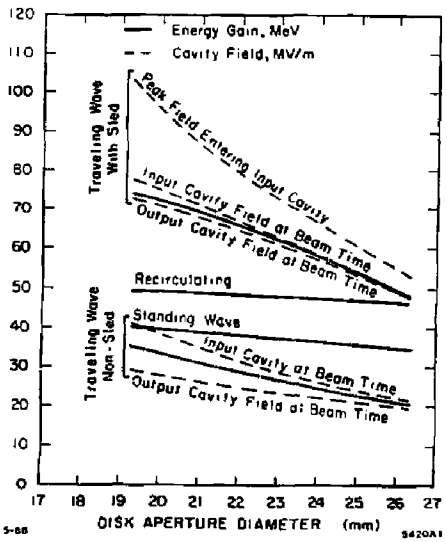


Fig. 1. Field and energy plots for 29-cavity constant-impedance structures at 2856 MHz driven by a 50 MW klystron through 0.97 dB loss.

## Design of Constant-Impedance Structure

*RF Design:*

Having established that a constant-impedance DLWG, operating TW and driven by a SLEDed klystron was the preferred system for our use, it remained to settle upon the structure length and the diameter of the disk aperture. All other dimensions, such as disk thickness and cavity length, were kept the same as in the standard SLAC constant-gradient accelerator section. The disk diameter was chosen to be 23 mm, being a compromise between the conflicting requirements of high shunt impedance and low wake-field excitation.

Some of the salient parameters of the structure at 2856 MHz are: $v_g/c = 0.0124$; $r_o = 57.0$ M$\Omega$/m; $\alpha = 0.177$; $Q_o = 13600$. Operating parameters for various lengths of the structure driven by a SLEDed 50 MW, 5 $\mu$s klystron pulse through 0.97 dB loss are given in Table I.

Figure 2 shows how, with SLED, the section energy and the input cavity field at beam time vary with section length.

*Work supported by the Department of Energy, contract DE-AC03-76SF00515.

*Contributed to the Stanford Linear Accelerator Conference, Stanford, California June 2-6, 1986*

**TABLE I**

| | | | | | | | |
|---|---|---|---|---|---|---|---|
| Section Length, | m | 0.5 | 1.0 | 1.5 | 2.0 | 2.5 | 3.0 |
| $T_f$, | ns | 134 | 269 | 403 | 538 | 672 | 807 |
| $\tau$, | nepers | .089 | .177 | .266 | .354 | .443 | .531 |
| SLED Energy-Gain | Factor | 2.44 | 2.32 | 2.21 | 2.10 | 2.00 | 1.90 |
| SLED Power-Gain | Factor | 6.49 | 6.45 | 6.40 | 6.34 | 6.29 | 6.22 |
| Non-SLED Energy, | MeV | 13.6 | 26.0 | 37.5 | 47.9 | 57.4 | 66.1 |
| SLED Energy, | MeV | 33.3 | 60.4 | 82.8 | 100.5 | 114.8 | 125.7 |
| Input Cavity Peak Field | MV/m | 72.4 | 72.2 | 71.9 | 71.5 | 71.3 | 70.9 |
| Input Cavity Field at Beam Time | MV/m | 65.9 | 59.9 | 54.3 | 48.6 | 44.2 | 39.2 |
| Output Cavity Field at Beam Time | MV/m | 66.2 | 60.5 | 55.1 | 50.2 | 45.8 | 41.7 |

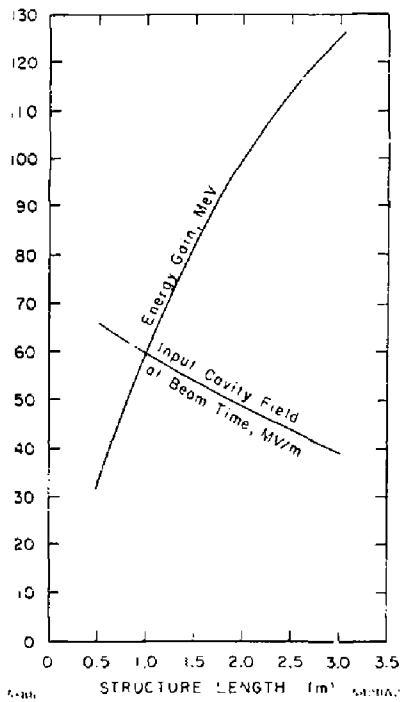


Fig. 2. Field and energy vs length, for constant-impedance DLWG structures driven by a SLEDed 50 MW klystron.

Another compromise had to be made, balancing the requirements of high energy gain and high fields in the input cavities. A length of 1.5 m was chosen. Figure 3 is a simple schematic of the high-power RF circuit, labeled to show the peak and average powers existing at various parts of the system.

*Thermal Considerations*

In operation, the 1.5 m section will be immersed in a shower-cone of electrons and positrons emanating from the target. The energy deposition resulting from this radiation has been computed using the Electron-Gamma Shower Program,

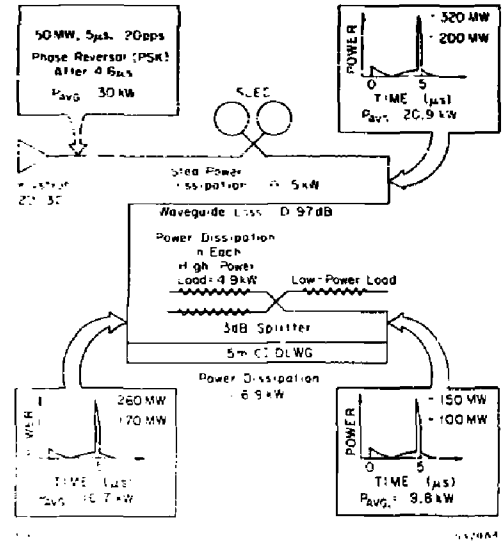


Fig. 3. Schematic of RF system, showing powers and waveforms.

Version 4. A typical set of shower trajectories computed by this program is shown in Fig. 4. For a 31.7 KW, 33 GeV electron beam incident on the target, the total radiation power dissipated in the 1.5 m section is calculated to be 12.6 KW. To this power must be added 6.9 KW of RF dissipation. Figure 5 shows the RF and radiation dissipation per cavity along the structure. Also plotted are the calculated metal and water temperature profiles along the DLWG cylinder, with RF only, and with radiation and RF. The water cooling system consists of 24 tubes uniformly spaced around the grooved periphery of the DLWG cylinder, and running parallel to the axis. The total water flow is 40 gpm.

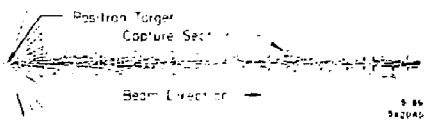


Fig. 4. Computed shower trajectories through capture section.

Using ETRANS, a program for tracing particles through an axially-symmetric magnetic field, it has been shown that the loss in positron yield resulting from an axial temperature gradient in the structure of 4°C will not be greater than 3.5%.

The RF and radiation losses in the first disk will be about 0.5 KW. With the cooling system described above, the radial temperature drop across the disk is calculated to be 19°C.

*Mechanical Design*

The constant-impedance disk-loaded structure was chosen in part because it is relatively simple to fabricate. The structure is a uniform stack of disks and spacers, aligned during brazing by means of stainless-steel pins fitted into precision-drilled holes. The input and output couplers have identical waveguide dimensions. The coupler cavity offset required

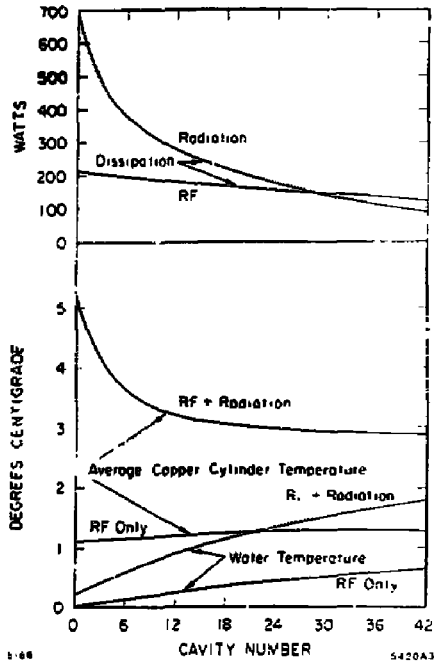


Fig. 5. Calculated heat dissipation and temperatures in capture section. Temperatures are referenced to the input water temperature.

to compensate for phase asymmetry was determined by interpolating between verified designs for other iris aperture diameters. Initial dimensions for the coupling iris and the coupler-cavity diameter were also obtained by interpolation.

Some complications were introduced by the water-cooling requirements and the need to have a quick-disconnect vacuum seal between the accelerator section and the target/flux-concentrator housing.

## Fabrication and Cold-Test

The disks and spacers were machined from OFHC copper. Critical dimensions were held to tolerances of ± 0.0002 inches. All internal surfaces have a 16 microinch finish (8 microinch finish on the critical disk aperture radii). In addition to mechanical quality-control inspection, each disk was clamped between two half-length spacers with closed end-plates, and the π-mode resonant frequency for the cell was measured. Resonant frequencies for all disks were required to lie within the range 2864.1 MHz ± 0.25 MHz. Similarly, each spacer was clamped between two end-plates, and the $TM_{010}$ resonant frequency of the cavity thus formed had to be 2876.4 MHz ± 0.25 MHz.

The correct dimensions for the coupler cavity diameter and coupling iris width were obtained by brazing the prototype coupler cavity to a stack of six of the standard CI cavities. (The diameter of the prototype cavity had been made slightly larger than what was estimated to be the correct value). The coupling iris was then machined in undersize (and therefore undercoupled). The correct dimensions were then set by the Khyl[4] method, knowing the $2\pi/3$ and $\pi/2$ frequencies for the CI stack.

The mid-section, comprising 30 CI cavities, was separately brazed together as a sub-assembly. This section was then joined to the identical input and output couplers in a separate brazing cycle. This operation was followed by machining the grooves for the water-cooling tubes. These tubes and their manifolds were then attached in a final braze run.

After this, the final tuning of the completed accelerator section was done. The section was purged with dry nitrogen, and water at a constant temperature of 28.5°C was circulated through the cooling system. Firstly, the input coupler match was checked by moving a short in the output waveguide by eighth-wavelength steps. Slight adjustments were made to the coupling and tuning to bring the Smith center and the Iconocenter to the center of the Smith Chart. Then, using the detuning plunger or nodal-shift technique, the structure cavities were dimple-tuned to give $2\pi/3$ phase-shift per cavity. At 2856 MHz, the final input and output VSWRs were both 1.03:1.

## High-Power RF Tests

The completed 1.5-meter section was temporarily mounted in the SLC positron source housing, in approximately the position it will occupy when permanently installed downstream of the target and flux-concentrator. It was supplied with RF power from a klystron at Station 20-3C, as shown schematically in Fig. 3.

The output power from the 1.5-meter section was divided between two high-power loads, which were of the standard SLAC tapered "sword" design. Dual-directional couplers, each with approximately −52 dB coupling, were incorporated in the waveguides at the input and output of the section. Separate water circuits cooled the waveguide feed, the 1.5-meter section and the output loads. Thermocouples and RTDs monitored metal and water temperatures. No temperature problems were anticipated or encountered with only RF dissipation, and no radiation heat load. A water-cooled copper plate formed the vacuum closure at the output end of the accelerator. This was intended to absorb the power from accelerated "dark current". No rise in temperature of this plate was recorded during the experiment. An ionization chamber mounted on axis a few inches downstream of the accelerator section monitored the radiation produced (see Fig. 8).

Initial RF processing was done with the SLED unit detuned. The klystron pulse width was 2.5 μs, and the repetition rate was 60 Hz. It took only a few hours of outgassing to reach 20 MW into the section, giving a peak axial field of 20 MV/m. After this, the peak and average powers were alternately increased by increasing pulse width and the repetition rate, and by tuning the SLED cavities. There were first run without phase-shift (PSK), to outgas the cavities and to provide intermediate levels of peak power to the accelerator section.

The peak SLED power ultimately delivered to the accelerator reached 168 MW, with the klystron providing 32.8 MW in a 5 μs flat-top pulse. The power into the accelerator was measured with a General-Microwave Model 478 Peak Power Meter, using a carefully calibrated coupler at the input to the accelerator, and a high quality coaxial line of known attenuation. Power measurements were double-checked, using other couplers in the system, and other recently calibrated power meters.

Installation schedules made it necessary to terminate the tests before processing was completed at the highest power level that the klystron could provide. The reflected energy fault rate at 120 Hz was still about 1 per minute, but the system was continuing to clean up. Gas pressures were falling, and the fault rate at 60 Hz was already down to 5 per hour. Processing up to higher powers was not possible because the XK-5 klystron available for the experiment saturated at 265 KV when delivering approximately 33 MW.

Figure 6 shows the RF input power waveform as measured at the output of the SLED cavities, at the beginning of the waveguide feed going to the accelerator section. Figure 7 is the expanded waveform of the SLED power peak entering the accelerator section. The peak power is 97.3 dB above 31.26 mW, i.e., 168 MW. The axial radiation due to captured and accelerated electrons created by field emission and residual gas ionization processes at the beginning of the accelerator section is plotted against input cavity peak RF power and axial field in Fig. 8. Measurements for curve (b) were taken about 4 hours later than for curve (a), showing how processing decreased the number of electrons available for acceleration.

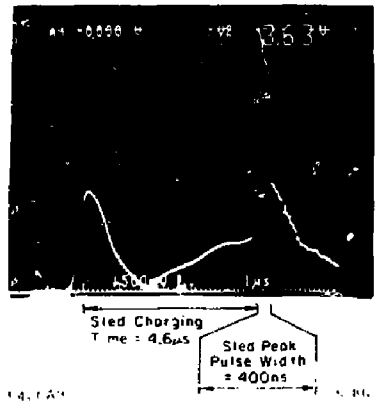


Fig. 6. RF power waveform measured at output of SLED cavities. The peak power is 210 MW.

## Conclusions

A traveling-wave, constant impedance disk-loaded waveguide section, 1.5 meters long, has been built for use as a high-field capture accelerator for the SLC Positron Source. It has been successfully tested up to the full power capability of a 33 MW SLEDed klystron, running at 120 Hz. At this level, the peak input power to the section was 168 MW, which is calculated to give 58 MV/m in the first cavity, and an average accelerating field of 43 MV/m.


## Acknowledgements

The authors would like to thank B. Smith for his excellent work on the mechanical design of the section. Thanks are equally due to H. Martin and P. Corredoura for their help in running the RF tests, and to the many members of the Mechanical Fabrication Department who contributed to the construction of the section.


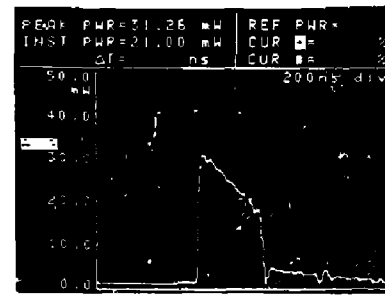


Fig. 7. SLED power peak entering the capture section.

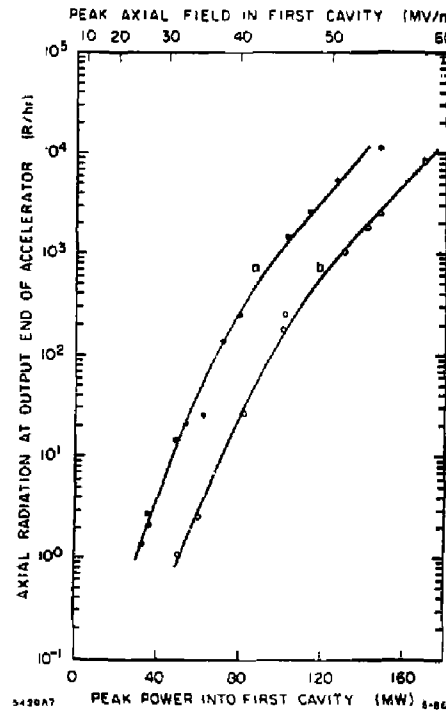


Fig. 8. Axial radiation as a function of peak power and axial field in first cavity of capture section. Curve (b) data taken four hours running time later than curve (a) data.

## References


1. F. Bulos *et al.*, *Design of a High Yield Positron Source*, IEEE Trans. on Nucl. Sci. NS-32, No. 5, 1985.
2. *Linear Accelerators*, edited by P. M. Lapostolle and A. L. Septier, Chapt. B.1.1., North Holland, 1970.
3. Z. D. Farkas *et al.*, *SLED: A Method of Doubling SLAC's Energy*, Proc. 9th Int. Conf. on High Energy Accelerators, 1974, p. 576.
4. E. Westbrook, *Microwave Impedance Matching of Feed Waveguides to the Disk-Loaded Accelerator Structure Operating in the $2\pi/3$ mode*, SLAC-TN-63-103, 1983.